Int. J. Electrochem. Sci., 16 **(2021)** Article ID: 21087, doi: 10.20964/2021.08.38

International Journal of
ELECTROCHEMICAL
SCIENCE
www.electrochemsci.org

Investigation of Anodic Behavior of Nickel in H_2SO_4 Solutions Using Galvanostatic Polarization Technique. IV. Initiation and Inhibition of Pitting Corrosion by Cl^- ions and Ethoxylated Surfactants

S. Abd El Wanees[1,2,*], *Ali.A. Keshk*[3]

[1] Chemistry Department, Faculty of Science, Zagazig University, Zagazig, Egypt.
[2] Faculty College of Umluj, Umluj, Tabuk University, Tabuk, Saudi Arabia.
[3] Chemistry Department, Faculty of Science, University of Tabuk, Tabuk, Saudi Arabia
[*]E-mail: s_wanees@yahoo.com, s_nasr@ut.edu.sa

Received: 6 April 2021 / *Accepted:* 21 May 2021 / *Published:* 30 June 2021

The anodic behavior of Ni in 0.01 M H_2SO_4 without and with the additions of NaCl was studied at a constant current density (2.6 $mAcm^{-2}$). The results depicted that the presence of Cl^- ions destroy the oxide layer and induce the pitting corrosion that depends on Cl^- ions concentration. The addition of some of the ethoxylated surfactants as inhibitors tolerates the destruction of the oxide layer and inhibits the localized pitting corrosion. Such surfactants shifted the E_{pit} towards the O_2 evolution potential and enhanced the rate of oxide film repair $(\partial E/\partial t)_i$ that depend on the surfactant type and amount. The inhibition efficacy of such compounds is dependent on the adsorption of such inhibitors on the Ni surface via electrons rich centers such as N and O atoms. The inhibition efficacy is based on an adsorption process that obeys Temkin's model by chemisorption mechanism. Some thermodynamic functions accompanied the pitting corrosion and adsorption of inhibitors were computed and explained. The surface morphology for some Ni samples in the aggressive and inhibitive solutions was investigated by SEM.

Keywords: Nickel; Ethoxylated Surfactant; Pitting; Adsorption; Inhibitor.

1. INTRODUCTION

The presence of chloride ions in an aqueous solution induces pitting corrosion for most metals and metal alloys [1-5]. A significant distinctive about pitting corrosion is the reality that pits can nucleate and grow at potentials beneath the pitting potential [5-11]. The localized pitting corrosion is depicted by various scenes, starting with the destruction of the passive layer, metastable pits creation followed by pit growth and propagation [5, 9, 10].

It is necessary to save the concerned metal against the destructive influence of the aggressive solution by adding ecofriendly inhibitors to the investigated environment. Generally, the most utilized inhibitors are hetero-organic molecules involving hetero-atoms such as O, N, and S in their structure [11-25]. The inhibition effect of most of the investigated molecules could be assigned to the existence of an adsorption process through the active sites on the investigated metal surface forming a protective layer that prevent the aggressive ions to attack the metal[19, 20].

Surfactant is regarded as one of the ultimate significant kinds of organic molecules due to the high inhibition influence towards the metal corrosion through their surface activity and adsorption capability for forming a preventative film on the metal surface. Furthermore, using of surfactants as inhibitors exhibits various advantages like its simplicity in the preparation in the laboratory and safety from environmental pollution [20–24]. The outstanding execution of surfactants as inhibitors towards the corrosion of most metals is realized almost to its adsorption ability through surface active centers inducing an insulating layer on the metal surface[24,25].

The present investigation aims to study the use of Cl^- as an aggressive ion to destruct Ni passivity and initiate the pitting corrosion in dilute sulfuric acid solution. The influence of three different types of ethoxylated surfactants as retarders towards the breakdown of passivity and initiate localized corrosion on nickel surface in dilute sulfuric acid solution containing Cl^- ions are examined using the galvanostatic polarization technique. The effect of temperature on the initiation of pitting corrosion was examined. Some of the thermodynamic parameters that accompanied the corrosion and adsorption processes are computed and explained. The surface morphology for some polarized Ni electrodes is investigated using the scanning electron microscope, SEM.

2. EXPERIMENTAL

2.1. Materials

The nickel electrode utilized in this study was a pure Ni rod. The procedure of preparing the working electrode has been described in the latest research and prepared as discussed in a recent work [5, 26]. The effective surface area of the nickel-metal exposed to the solution was 0.97 cm^2. Before each test, the working Ni-electrode area was mechanically polished employing different grades of fine emery papers. After polishing the Ni- electrode was cleaned by rapid washing using rinsing with propanone and bi-distilled and directly immersed in the examined solution.

The utilized inhibitors are N-ethoxylated(n)bis[N-ethyl-p-dodecylbenzenesulphonamide] with various chains of ethylene oxide units. The experimental procedure used to prepare these inhibitors is the same described before [20]. The sulfonamide compound is prepared by refluxing dodecyl benzenesulfonic acid with diethylenetriamine, at 140 °C. The product is ethoxylated using ethylene oxide to obtain the required surfactants with different ethylene oxide units (n = 5, 10, and 15) [20, 27], Scheme 1.

The investigated solutions were prepared using A.R. sulphuric acid, NaCl (Fluka), and double-distilled water. Experiments are carried at 25°C, except for those experiments that are done at different temperatures. The surface morphology is carried out utilizing SEM, JEOL TM, JSM- T100 (Japan).

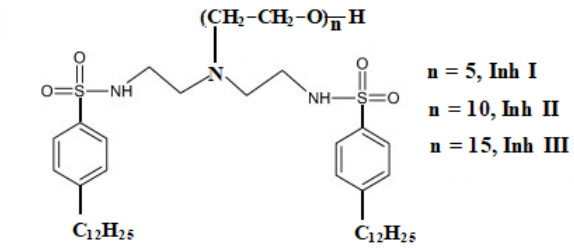

Scheme 1. N-ethoxylated(n)bis[N-ethyl-p-dodecylbenzenesulphonamide], when n = 5, Inh I, n = 10, Inh I, and n = 15, Inh III

2.2. The Electrolytic cell

The description of the polarization cell was reported before [26, 28]. The required electrodes are Pt-wire (Auxiliary electrode), Ni (working electrode), and a calomel, SCE (reference electrode). A Luggin capillary is focused on the Ni electrode surface to avoid the pseudo-ohmic potential. Before running the anodic process, the Ni electrode was subjected to a cathodic current for about 15 min in the investigated solution with the applied polarizing current density (2.60 mA/cm^2 to reduce any pre-immersion oxide films that are formed on the metal surface). The polarizing current was then reversed in the anodic direction and the potential, *E* was followed as against the reaction time, *t*. Electrolytic solutions were prepared from analytical grade reagents and bi-distilled water. Experiments were carried out at a constant temperature, 25$\pm$ 1°C, except those related to the effect of temperature. The cell temperature was controlled using an ultra-thermostat, Polyscience (USA). Each experiment was carried out in a freshly prepared solution and with a newly polished electrode surface. Polarization curves were recorded on a recording unit, Cole Parmer Instrument. The quantity of electricity, Q consumed in the initiation of pitting corrosion can be calculated from the product of the value of the polarizing current multiply, 2.60 mA/cm^2 by the time required to initiate the pitting corrosion. The rate of oxide film repair can be deduced from the slope value of the potential-*t* rise in the passive region (zone III).

3. RESULTS AND DISCUSSION

3.1. The effect of NaCl additions

Fig 1 shows the galvanostatic anodic polarization data (*E-t*) of Ni electrodes in 0.01 M H_2SO_4 devoid of and containing different amounts of Cl^- ions, at 2.6 mA/cm^2 and 25^{o}C. The polarization curves of the investigated solutions are identified by a fast skip of potential (zone I) emphasizing the

decay of H_2 overpotential pursued by charging of the electrical double layer [5, 26, 28]. After that, the sweep in the potential, *E*, becomes slow till the appearance of the humps ***x*** and ***y*** (zone II) pursued by a potential rise again (zone III), owing to the formation of the passive layer region, before reaching the potential of O_2 evolution, as shown in the case of Cl^- ions-free solution, curve 1 in Fig 1.

Little amounts of Cl^- ions (< 0.00025 M) do not affect the polarized curve obtained in Cl^- ions-free solution. Increasing the amounts of Cl^- to 0.00025 M or more deform the polarized curve owing to the destruction of the passive layer and formation of metastable pits, at E_{pit} [29-31]. The initiation of pitting corrosion can proceed easily which increases with the additions of Cl^- ions [28,31, 32].

However, the existence of Cl^- ions enhances the active metal dissolution by shifting the oxidation potentials, arrests ***x*** and ***y***, into a more negative direction with the destruction of the oxide layer at the pitting potential, E_{pit}, curves 2-7, Fig 1 [28]. The regions I and II of curves 2-7 correspond in resemblance with that of the Cl^- ions-free solution. The existence of Cl^- ions decrease the rate of oxide film building, $\partial E/\partial t$, region III, with a lowering in the E_{pit} values (Fig 2), owing to the enhancement of the pitting corrosion [28]. However, the existence of vacillation after E_{pit}-region (in Zone III) could be attributed to the competition between the oxide film destruction by Cl^- ions and oxide film repair by water molecules[31].

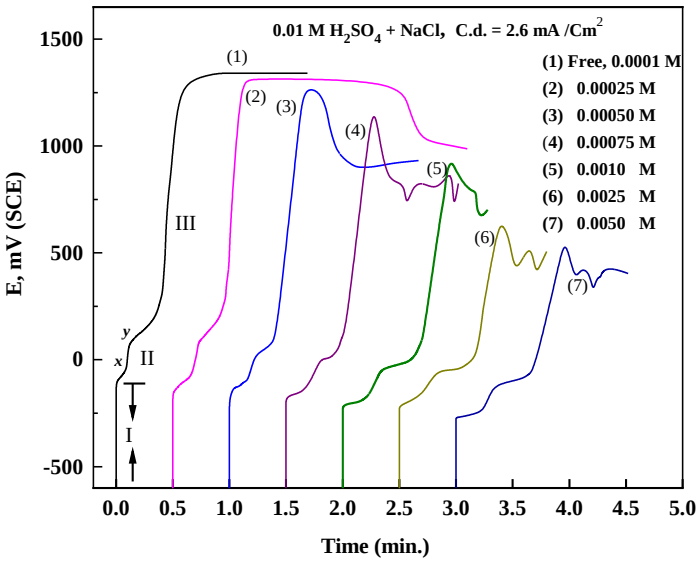

Figure 1. The anodic polarization data, *E*-time curves of Ni in 0.01 M H_2SO_4 containing various concentrations of NaCl, at 1.0 mA/cm^2 and 25^{o}C.

The shift of the E_{pit} into the lower values with raising the additions of Cl^- ions is depicted in Fig 3. Segmented S-shape curves are obtained explaining the variation of E_{pit} with the log C_{Cl^-}. Such relation is similar to an adsorption isotherm form which can confirm the adsorption of Cl^- ions on the Ni surface during the pitting corrosion process [32]. The displacement of E_{pit} values into more active values could be considered as evidence of the promotion of pitting corrosion with more additives of Cl^- ions. Fig 4 confirms the rise in the quantity of electricity, Q, consumed for the destruction of the oxide layer with the initiation of the localized corrosion on nickel in sulfuric acid polluted with Cl^- ions.

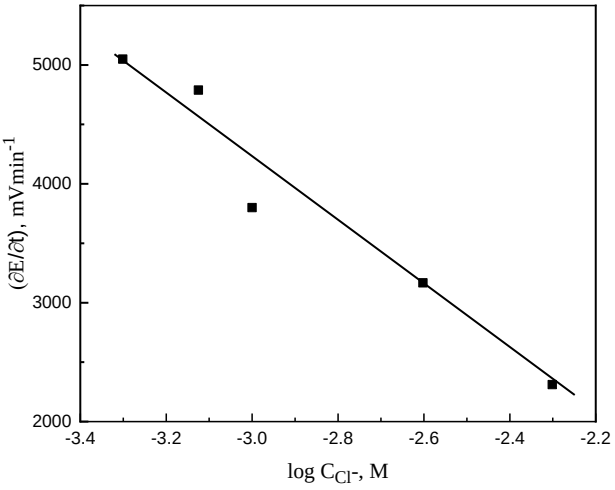

Figure 2. The dependence of $(\partial E/\partial t)_i$ on the logarithmic concentration of Cl^- ions, C_{Cl^-} for nickel in 0.01 M H_2SO_4, at 25ºC.

The surface micrograph of the investigated on Ni-sample (after carrying the polarization experiment for nickel electrode in sulfuric acid mixed with 0.005M Cl^-) is shown in Fig 5. The image elucidates some different sizes of extended pits surrounded by corrosion products on the nickel surface. The appearance of various size pits surrounded by some of the corrosion products is evidence of localized pitting corrosion and the damage of the passive oxide layer that formed on the nickel surface with the initiation of pitting corrosion.

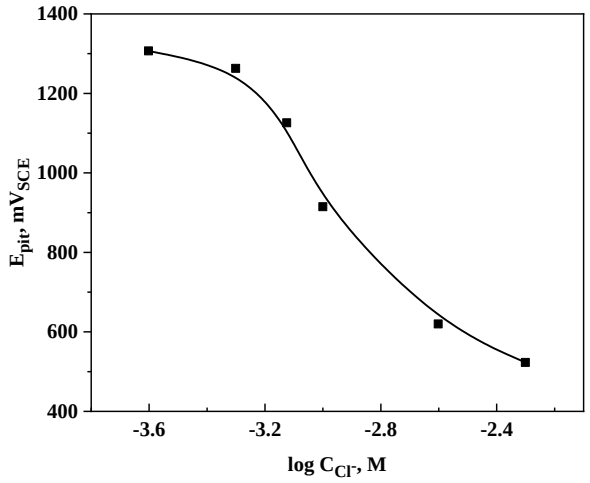

Figure 3. E_{pit} -log C_{Cl^-} relation for pitting corrosion of Ni in 0.01 M H_2SO_4, at 25ºC.

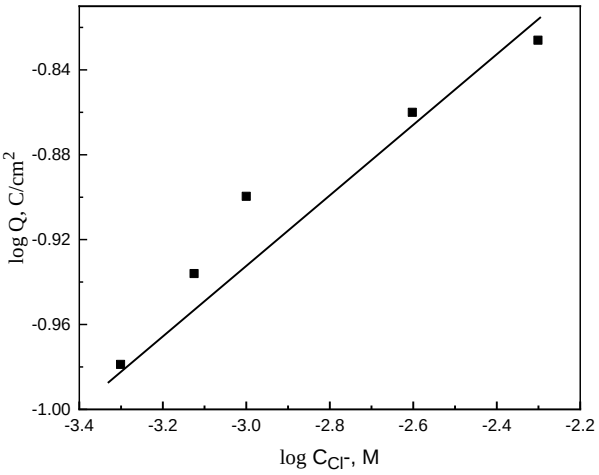

Figure 4. The dependence of the quantity of electricity for pit initiation, log *Q*, on the amount of Cl^- ions, log C_{Cl^-} for nickel in 0.01 M H_2SO_4, at 25°C.

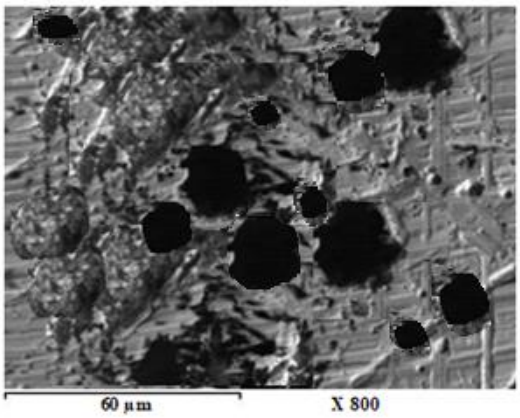

Figure 5. SEM micrograph of Ni sample after the polarization in 0.01 M H_2SO_4 mixed with 0.005M Cl^- ions.

3.1. The influence of inhibitor addition

Fig 6 depicts the anodic polarization data of nickel electrodes in 0.01M sulfuric acid solution mixed with 0.005 M Cl^- ions devoid of and containing various amounts of Inh III. Similar data are gained when Inh I and Inh II are added (curves not shown). For all added inhibitors the curves have a similarity in the characterization regions (zones I and II). The exception in the similarity between the curves is the passive region (zone III). The existence of the surfactant inhibitor in the examined solution shifts the E_{pit} into the more noble values due to the toleration of the pitting corrosion.

However, the curves of Fig 6 depict that the addition of few amounts of surfactant displaces the E_{pit} into less active values towards the oxygen evolution region. Additions of 1 $x10^{-5}$ M of Inh III displaces the E_{pit} from 525 mV_{SCE} into 582 mV_{SCE}, whilst $1x10^{-2}$ M of Inh III prevents the pitting corrosion to occur by displacement the electrode potential into 980 mV_{SCE}.

It is noted that the release of fluctuations in the polarized curves after the pitting potential region can be elucidated by the competition action between the Cl^- ions as destructive anions and the inhibition influence of surfactant molecules towards the metal surface. The higher addition of surfactants blocks the formed metastable pits and prevents the propagating of pitting corrosion by raising the rate of oxide film repair [31].

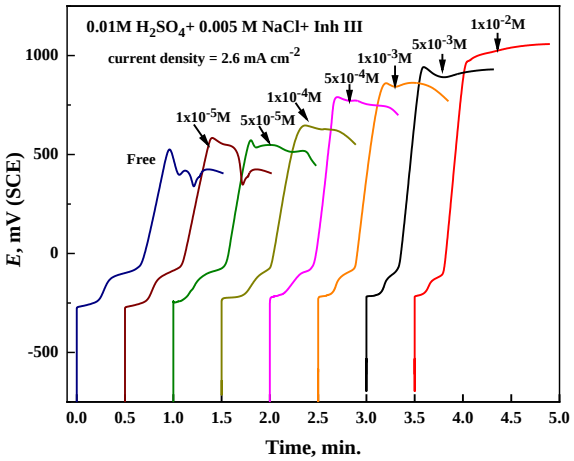

Figure 6. The anodic polarization data, *E*-time curves for nickel in 0.01 M H_2SO_4 mixed with 0.005 M NaCl without and with various amounts of Inh III, at 2.6 $mAcm^2$ and 25 ^oC

The variation of the E_{pit} values with the logarithmic concentration, log C_{inh} of the used surfactant molecules is shown in Fig 7. S-shaped curves analogous to the adsorption curves are obtained. The E_{pit} rises with raising the amount of the added surfactant confirming the adsorption of such molecules on the Ni surface prohibiting metastable pits formation [31]

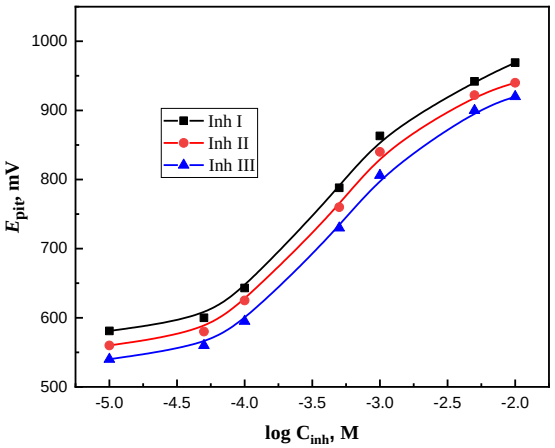

Figure 7. Dependence of E_{pit} on the inhibitor amount, log $C_{inh,}$ for nickel in 0.01 M H_2SO_4 mixed 0.005 M NaCl, at 25^oC.

The rate of oxide-film repair, $(\partial E/\partial t)_i$ obtained from the slope value of the potential-*t* rise in the passive region (zone III Fig 6) is found to increase with the added amounts of surfactant according to the S-shaped curve, Fig 8. Such attitude is attributed to the probability of the existence of an adsorption step confirming the inhibition effect of the surfactant molecules on the Ni surface[31].

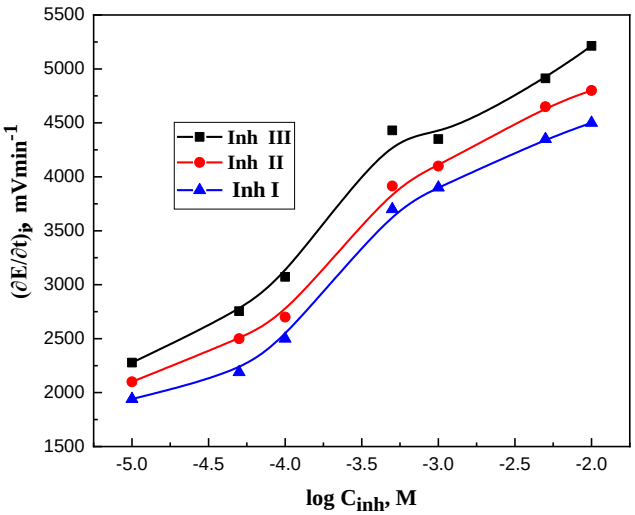

Figure 8. The dependence of $(\partial E/\partial t)_i$ on the log C_{inh} for nickel in 0.01M H_2SO_4 and 0.005 M NaCl, at 25°C.

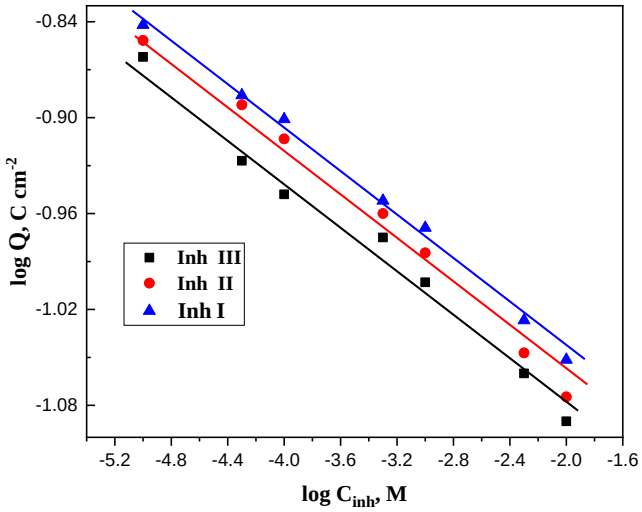

Figure 9. Double logarithmic relation between the quantity of electricity (Q) and inhibitor concentration, C_{Cl^-}, for nickel in 0.01M H_2SO_4 mixed with 0.01 M NaCl.

Fig 9 indicates the relation between the quantity of electricity (log Q) required to damage the oxide film and initiate the localized pitting on the Ni surface with the amount of the added surfactant (log C_{inh}) in 0.01M sulfuric acid solution mixed with 0.01 M Cl^- ions. The amount of Q required for

the initiation of pitting corrosion relies on the inhibitor kind and decreases as the inhibitor concentration is raised. Such attitude confirms the inhibition influence of the used inhibitors toward the pitting corrosion of Ni.

The surface morphology of the examined Ni-sample in 0.01 M sulfuric acid mixed with 0.005M Cl^- and 0.0001 M of Inh III is shown in Fig 10. The image indicates a smooth surface with some scratches free from any pits, which confirms the inhibition effect of the used inhibitor molecules towards the pitting corrosion of Ni.

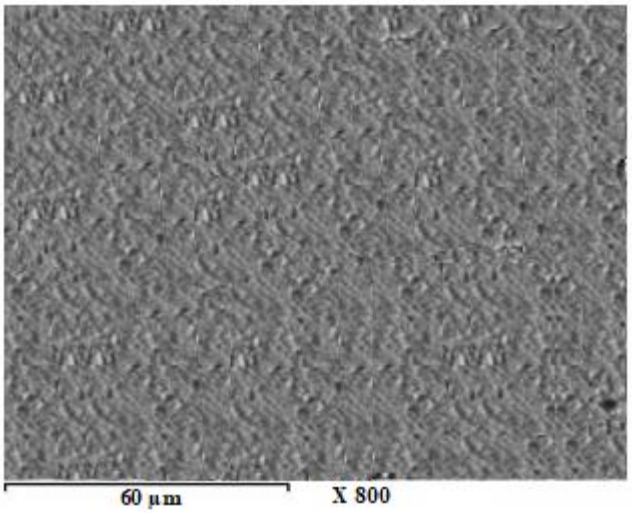

Figure 10. SEM micrograph for Ni sample after polarization in 0.01 M H_2SO_4 mixed with 0.005 M Cl^- and 0.0001 M of Inh III.

The inhibition efficacy, η %, of inhibitors towards the destruction of the oxide film and the initiation of the localized corrosion and can be computed from the quantity of electricity required to initiate the localized corrosion during polarization experiments, following the equation:

$$\eta\,\% = \left(1 - \frac{Q_{inh}}{Q_{free}}\right) x100 \qquad (1)$$

where Q_{free} and Q_{inh} are the quantities of electricity in 0.01M sulfuric acid solution mixed with 0.01 M NaCl devoid of and containing the surfactant, respectively. The inhibition efficacies of the different surfactants towards the pitting corrosion of Ni are recorded in Table 1. It is found that η % depends on the inhibitor kind and its amount in the solution. The inhibition efficacy towards the pitting corrosion of different surfactants on Ni in 0.01M sulfuric acid solution mixed with 0.01 M NaCl decreases in the order: Inh III > Inh II > Inh I. This sequence emphasizes the increased propensity of the used surfactants as inhibitors towards pitting corrosion as the number (n) of ethylene oxide units increase in the molecule. Early, It is suggested that the inhibition of Zn corrosion in HCl was dependent on the number of repetitions of ethylene oxide units in the molecule [20]. Inh III exerts higher inhibition efficacy (n = 15) than that of Inh II (n = 10) and Inh I (n = 5). A higher number of ethylene oxide units in the surfactant molecules increases the number of adsorption sites as attributed

to the increase in the number of O-atoms in the molecule which sustains the formation of an isolating layer on the metal surface preventing Cl^- ions to attack the metal surface [20]. Also, one cannot ignore the effective role of the N and S atoms besides the π −bonds of the benzene ring as electrons donors forcing the adsorption of such molecules to takes place on the metal surface. The adsorbed surfactant molecules could be combined into the passive film enhancing the oxide film repair against the aggressive influence of Cl^- ions [32, 33].

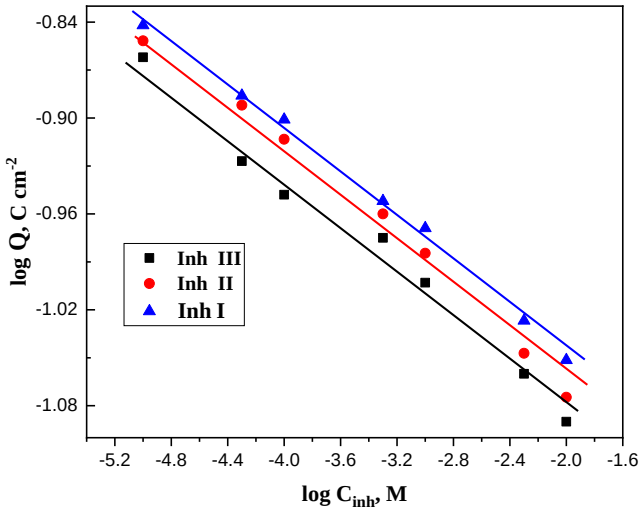

Figure 11. Dependence of Q on the inhibitor amount, C_{inh} for Ni in 0.01M H_2SO_4 mixed with 0.005 M Cl^-.

Table 1. The values of the inhibition efficiency for different inhibitors towards the pitting corrosion of Ni in 0.01 M H_2SO_4 containing 0.005 M NaCl solutions at 25 ◦C.

Concentration, M	the inhibition efficiency, η %		
	Inh I	Inh II	Inh III
$1x10^{-5}$ M	03.0	5.0	07.1
$5x10^{-5}$ M	11.8	13.5	16.2
$1x10^{-4}$ M	15.2	17.5	20.0
$5x10^{-4}$ M	24.5	26.0	28.4
$1x10^{-3}$ M	27.4	30.0	33.0
$5x10^{-3}$ M	36.3	39.4	41.7
$1x10^{-2}$M	40.0	43.1	45.5

3.2. Adsorption isotherm

Generally, the first step in the inhibition of metal corrosion is the adsorption of the organic molecules on the metal interface, $OM_{(ads)}$. The inhibition efficacy of such molecules relies on the homogeneity of the metal surface as well as the surface coverage, θ, of the corroded metal surface. The adsorption of inhibitor molecules is a quasi-substitution process between the surfactant molecules, $OM_{(sol)}$, and $H_2O_{(ads)}$ on the corroded metal surface.

$$OM_{(sol)} + H_2O_{(ads)} \leftrightarrow OM_{(ads)} + x\ H_2O_{(sol)} \quad (2)$$

where x is the size ratio that represents the number of H_2O molecules substituted by one inhibitor molecule.

The surface coverage, θ, is computed from the corrosion rate values (expressed by the quantities of electricity required to destruct the passive film in the absence and presence of surfactant). The data are employed to fit the various forms of the adsorption isotherm equations. The Temkin adsorption model was suitable and adequate to fit the obtained data with a correlation coefficient (r^2) very near to 1, as depicted in Fig. 12. The Temkin equation can be expressed by the following relation:

$$\exp(-2a\theta) = K_{ads}\, C_{inh} \quad (3)$$

$$\theta = -\frac{1}{2a}\ln K_{ads} - \frac{1}{2a}\ln C_{inh} \quad (4)$$

where C_{inh} represents the surfactant amount, a is the lateral interaction parameter depicting the molecular interaction and the heterogeneity of the corroded metal surface, and K_{ads} represents the adsorption-desorption equilibrium constant of inhibitor molecules. The positive value of a confirms the existence of attractive forces between the adsorbed inhibitor molecules. A negative value of a supposes the presence of repulsion force between the adsorbed molecules [34, 35]. The computed values of "a" are −9.01 and −9.03, and -9.35 for Inh III, Inh II, and Inh I, successively. Such a conclusion confirms the existence of repulsion forces between the adsorbed surfactant molecules on the Ni surface[35,36]. Moreover, the computed K_{ads} values are 36.6×10^4 L/mol, 23.3×10^4 L/mol, and 17.8×10^4 L/mol for Inh III, Inh II, and Inh I, successively. A higher K_{ads} is correlated with the more adsorption capacity of the surfactant molecules on the nickel surface [37,38]. Thus, inhibitor Inh III has a higher adsorption ability on the nickel surface.

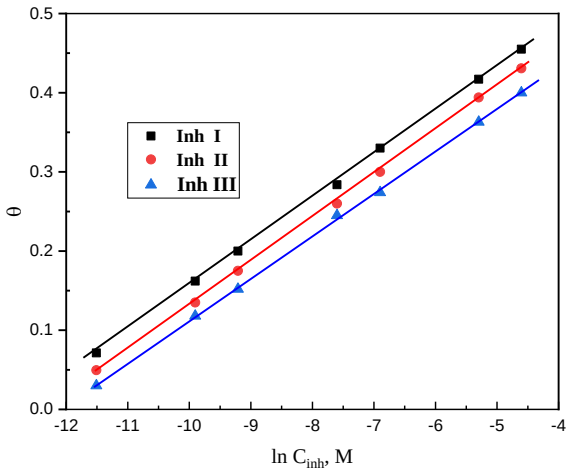

Figure 12. Temkin adsorption isotherm for different inhibitors on Ni in 0.01 M H_2SO_4 containing 0.005 M NaCl

The free energy of adsorption, ΔG^{0}_{ads}, is a thermodynamic function needed to designate the adsorption process and can be computed from K_{ads} values according to the relation[20, 26]:

$$\Delta G^{\circ}_{ads} = -RT \ln (55.5\, K_{ads}) \quad (5)$$

where R is the ideal gas constant, T is the absolute temperature, and 55.5 is the molar concentration of water in mol/L in the solution. The standard Gibbs free energy characterized by a negative value is correlated with the spontaneous adsorption process and the stability of the adsorbed layer formed on the nickel surface. Commonly, ΔG^{0}_{ads} values around or more than −20 kJ/mol are associated with the Vander Walls forces of interaction (physisorption mechanism) due to the electrostatic attraction among surfactant molecules and the charged Ni surface. On the other hand, chemisorption is accompanied by ΔG°_{ads} values around or less than −40 kJ/mol. In the chemical adsorption mechanism, electrons are transferred or shared from the inhibitor molecules to the metal surface to form a coordinate-type bond [39-42]

The values of ΔG°_{ads} of Inh III, Inh II, and Inh I are −31.74, -30.62, and −29.95 kJ/mol, respectively, Table 2. This conclusion proves that the inhibition of the used inhibitor molecules towards the pitting corrosion on the nickel surface is completed via the chemisorption mechanism. Inhibitor I has a high ability to form a stronger bond with the Ni surface than other inhibitors. The ΔG°_{ads} values with negative signs emphasize the spontaneity of the adsorption process for the surfactant molecules on the nickel surface. Mostly, ΔG°_{ads} values up to -20 kJ/mol are compatible with the physisorption model. On the other hand, ΔG°_{ads} values ≤ - 40 kJ/mol are consistent with the chemical adsorption mechanism owing to the chemical bond formation by sharing or transfer of electrons between the inhibitor molecules and the metal surface via electrons density on the active sites of the adsorbed molecules [43].

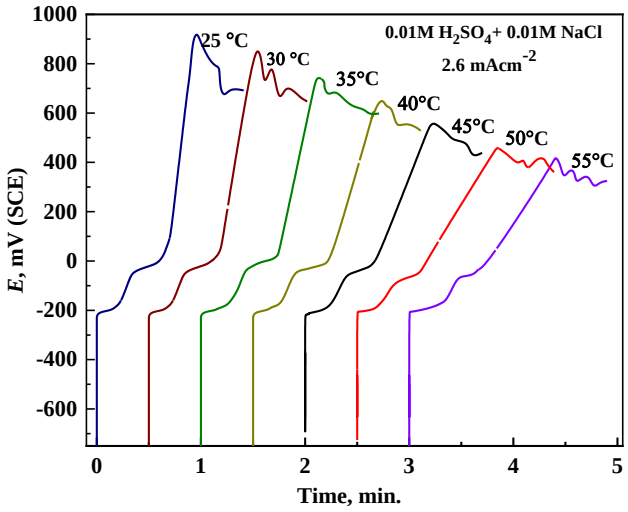

Figure 13. The influence of temperature on the *E*-time curves of nickel in 0.01 M H_2SO_4 mixed with 0.01 M NaCl and $1x10^{-4}$ M of 3-allyl-1-[(2-methoxyphenyl)methyl]thiourea.

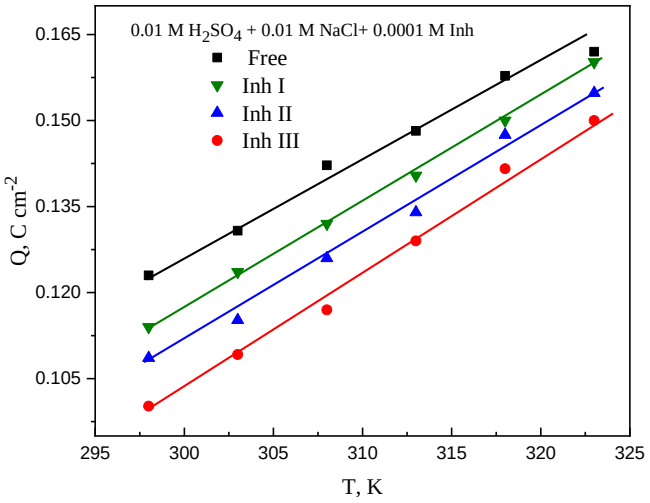

Figure 14. The dependence of *Q* on the temperature, *T*, for nickel in 0.01 M H_2SO_4 mixed with 0.01 M NaCl and 0.0001 M inhibitor.

3.3. The influence of temperature

The influence of temperature on the anodic polarization of nickel in 0.01M sulfuric acid solution mixed with 0.005 M Cl^- ions without and with 0.0001 M of the surfactant was examined.

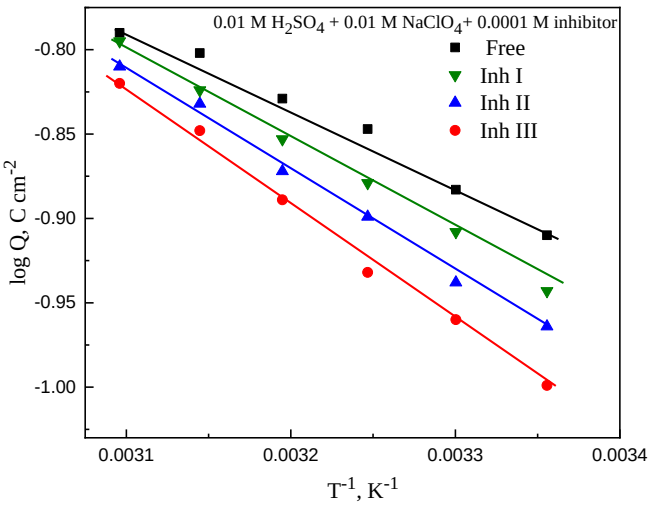

Figure 15. Arrhenius plots for Ni in 0.01M H_2SO_4 mixes with 0.01 M NaCl and 0.0001 M inhibitor.

Fig 13 represents the anodic polarization data of Ni in the sulfuric acid solutions contaminated with 0.005 M NaCl at different temperatures. Analogous curves are obtained in 0.01M sulfuric acid

solution mixed with 0.005 M Cl^- ions and 0.01 M of the surfactant (curves not shown). Fig 13 and the similar ones indicated that the increase in the solution temperature elongates the time of the active oxidation of Ni and passive film formation with shifting of E_{pit} into the active direction due to the initiation of the localized corrosion. The rate of oxide film repair (region III), $\partial E/\partial t$, is reduced with increasing the temperature. The increase in the time of Ni oxidation and the reduction in the rate of oxide film repair by the temperature can be related to the increase in the mobility of ions by temperature[44]. The quantity of electricity required to initiate the pitting corrosion and damage the oxide film, Q, is found to increase with absolute temperature, Fig 14.

The activation energy, E_a, for the pitting corrosion of Ni can be determined using the Arrhenius relation[45-47]:

$$\log\ Q = \frac{-\Delta H_a^\circ}{2.303\ RT} + \log A \qquad (6)$$

where Q represents the quantity of electricity required to initiate the pitting corrosion, T is the absolute temperature, A is the Arrhenius constant and R is the gas constant (8.314 J $K^{-1}mol^{-1}$).

The values of log Q are plotted against the inverse of absolute temperature,1/T, Fig 15. The activation energies for the pitting corrosion, E_a were computed from the slope values, Table 2. The value of E_a, for the initiation of pitting corrosion of nickel in 0.01 M sulfuric acid solution containing 0.005 M NaCl was 9.7 kJ/mol [6]. In the presence of 0.001 M inhibitors, the calculated values of E_a are increased to be 12.1, 14.5, and 16.4 in the case of Inh I, Inh II, and Inh III. The rise in E_a values in the presence of inhibitors is attributed to the increase in the energy barrier of the formed insulating layer, which suggests a physical adsorption process.

The enthalpy, ΔH_a, and entropy, ΔS_a, of activation of oxide film damage and initiation of pitting corrosion can be determined from the transition state equation [45-47]

$$r = \frac{RT}{Nh}\ exp\left(\frac{\Delta S_a^\circ}{R}\right)\ exp\ (\frac{-\Delta H_a^\circ}{RT}) \qquad (7)$$

where R represents the ideal gas constant, h and N are the Plank's and Avogadro's constants, ΔH_a° is the enthalpy of activation, while ΔS_a° is the entropy of activation. Fig 16 represents the plots of log (Q/T) versus 1/T in case of the destructive solution (0.01 M sulphuric acid containing 0.005 M NaCl) and the inhibitive solution (0.01 M H_2SO_4 + 0.005 M NaCl + 0.0001 inhibitor) . Fig 16 gives straight-line relations confirming the transition state plots of equation 6. The enthalpy of activation ΔH_a° and the entropy of activation ΔS_a° values are determined from the slopes, $-\Delta H_a^\circ/2.303R$ and the intercept, log(R/hN) + $\Delta S_a^\circ/2.303$ R), successively, and are represented in Table 3. The values of ΔH_a° characterized by positive sign reflects the endothermic nature of the destruction process in each of the aggressive and inhibitive solutions. On the other hand, the increase in the ΔS_a° values in the presence of the surfactants inhibitors can be related to the increase in the degree of the disorder when the reactants pass to the activated complex, which is attributed to the increase of inhibitor molecules covering the surface in the determining state.

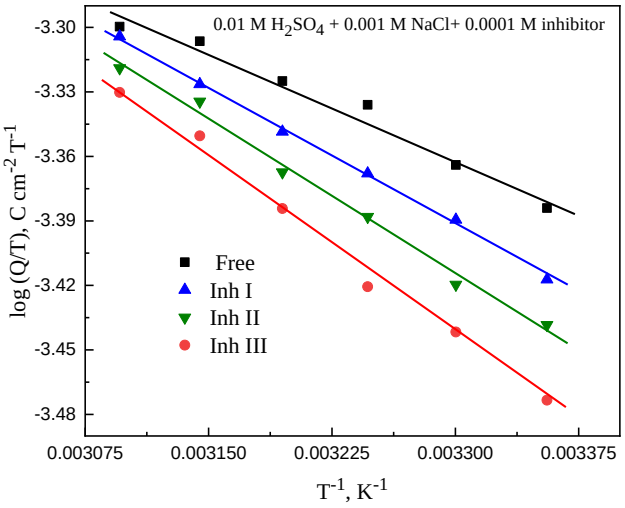

Figure 14. Transition state plots for Ni in 0.01M H_2SO_4 mixed with 0.005 M NaCl without and with 0.0001 M of different inhibitors.

Table 3. Thermodynamic corrosion parameters, the activation energy for pitting corrosion, E_a, enthalpy, and entropy of Ni in 0.01 M H_2SO_4 mixed with 0.005 M NaCl and 0.0001 M inhibitors.

Type of anions	E_a, kJ mol^{-1}	ΔH, kJ/mol	-ΔS, J/mol
0.01 M ClO_4^-	9.39	6.49	-238
0.01 M ClO_4^- + 0.0001 M Inh III	10.50	8.15	-235
0.01 M ClO_4^- + 0.0001 M Inh II	11.74	9.20	-232
0.01 M ClO_4^- + 0.0001 M Inh I	13.40	10.84	-228

4. CONCLUSION

The electrochemical behavior of nickel in 0.01 M H_2SO_4 polluted with Cl^- ions without and with the additions of various types of ethoxylated surfactants as inhibitors signalized that:

i- Various amounts of Cl^- ions damage the oxide layer and initiate the localized pitting Corrosion type, at E_{pit}.

ii- The inhibitor molecules enhance the oxide film repair, $(\partial E/\partial t)_i$, and displace the E_{pit} into the more positive values.

iii- The inhibition of pitting corrosion could be assigned to the adsorption of the surfactant molecules on the Ni surface.

iv- The inhibition efficacy increases with increasing the number of repeated ethylene oxide units in the ethoxylated surfactant molecules.

v- The adsorption of the surfactant molecules obeyed the Temkin adsorption isotherm through combined physical and chemical interactions

References

1. S. Abd El Wanees, A.A. El Aal, E.E.El Aal, *Br. Corros. J*., 28 (1993), 222.
2. S.M. Abd El Haleem, S. Abd El Wanees, E.E. Abd El Aal., A. Farouk, *Corros. Sci*., 68 (2013)1.
3. S.M. Abd El Haleem, S. Abd El Wanees, E.E. Abd El Aal, A. Diab, *Corros. Sci*., 52 (2010) 292.
4. S. Abd El Wanees, A.B. Radwan, M.A. Alsharif, S.M. Abd El Haleem, *Mater. Chem. Phys*., 190 (2017) 79.
5. S. Abd El Wanees, M. Abdallah, A.S. Al-Gorair, F.A.A. Tirkistani, S. Nooh, R. Assi, *Int. J. Electrochem. Sci*., 16 (2021) 150969.
6. G.T. Burstein, S.P. Mattin, P.C. Pistorius, *Corros. Sci*., 35 (1993) 57.
7. G. T. Burstein, Souto R.M., *Electrochim. Acta,* 40 (1995) 1881.
8. H.S. Isaacs, *Corros. Sci*., 29 (1989) 313.
9. P.C. Pistorius, G. T. Burstein, *Philos. Trans., Roy. Soc*., 341(1992) 531.
10. S. Abd El Wanees, A. Abd El Aal, M. Abd El Azeem and A.N. Abd El Fatah, *Int.. J. Electrochem. Sci.*, 3 (2008) 1005.
11. E.E. Abd El Aal, S. Abd El Wanees, *Corros. Sci*., 51 (2009) 1780.
12. Abdallah M., Zaafarany I., Abd El Wanees S., Assi R., *Int. J. Corros. Scale Inib*., 4 (2015) 338.
13. S. Abd El Wanees, E.E. Abd El Aal, *Corros. Sci*., 51 (2009) 1611.
14. M. Abdallah, S. Abd El Wanees and R. Assi, *Port. Electrochim. Acta*, 27 (2009)77.
15. S. Abd El Wanees, M.I. Alahmdi, M. Abd El Azzem, H.E. Ahmed, *Int. J. Electrochem. Sci*., 11 (2016) 3448.
16. S Abd El Wanees, *Anti-Corros. Meth. Mater*.. 4 (1994) 4.
17. S. Abd El Wanees, E.E. Abd El Aal, A. Abd El Aal , *Bull. Soc. Chim. Fr*., 128 (1991) 889.
18. S. Abd El Wanees, M.I. Alahmdi, M.A. Alsharif, Y. Atef, *Egypt. J. Chem*., 62 (2019) 811.
19. S. El Wanees, A.A.H. Bukhari, N.S. Alatawi, S. Salem, S. Nooh, S.K. Mustafa, *Egypt. J. Chem*., 64 (2021) 547.
20. S. Abd El Wanees, N.M. ElBasiony, A.M. Al-Sabagh, M.A. Alsharif, S.M. Abd El Haleem, M. Migahed. *J. Mol. Liq*., 248 (2017) 943.
21. A.G. Bedir, A Abd El-raouf, S. Abdel-Mawgoud, N. A. Negm, N.M. ElBasiony , *ACS Omega,* 6 (2021) 4300.
22. F.H. Al-Abdali, M. Abdallah, R. El-Sayed, *Int. J. Electrochem. Sci.*, 14(2019) 3509.
23. A. M. Al-Sabagh, N. M. Nasser, O. E. Al-Azabawy, A.E. Tabey, *J. Mol. Liq.*, 219 (2016) 1078.
24. A.M. Alsabagh, M.A. Migahed, H.S. Awad, *Corros. Sci*., 48 (2006) 813.
25. M.A. Migahed, M. Abd-El-Raouf, A.M. Al-Sabagh, H.M. Abd-El-Bary, *Electrochim*. Acta, 50 (2005) 4683.
26. S. Abd El Wanees, A. S. Al-Gorair, H. Hawsawi, S. S. Elyan, M. Abdallah, *Int. J. Electrochem. Sci.,* 16 (2021) 210548.
27. A.N. Wrigley, F.D. Smith, A.J. Stirton, *J. Am. Oil Chem. Soc.*, 34 (1957)39.
28. F. M. Abd El Wahab, J. M.Abd El Kader, H.A. El Sayed, A.M. Shams El-Din, *Corros. Sci*., 18 (1978) 997.
29. E.E. Abd El Aal, S. Abd El Wanees, *Corros. Sci*., 51 (2009) 458.
30. S. M. Abd El-Haleem, S. Abd El-Wanees, *Mater. Chem. Phys*., 128(2011) 418.
31. E.E. Abd El Aal, *Corros. Sci*., 45 (2003) 759.
32. S.M. Abd El Haleem, S. Abd El Wanees, E.E. Abd El Aal, A.Farouk, *Corros. Sci.* 68 (2013)1.
33. S.M. Abd El Haleem, S. Abd El Wanees, E.E. Abd El Aal, A. Diab, *Corros. Sci*., 52 (2010) 292.
34. S. Qian, Y.F. Cheng, *J. Mol. Liq*., 294 (2019) 111674.
35. S. Umoren, E. Ebenso, *Mater. Chem. Phys*., 106 (2007)387.
36. L. Tang, X. Li, Y. Si, G. Mu, G. Liu, *Mater. Chem. Phys*., 95 (2006)29.
37. Z. Hu, Y. Meng, X. Ma, H. Zhu, J. Li, C. Li, D. Cao, *Corros. Sci*., 112 (2016)563.
38. S. Refaey, F. Taha, A.A. El-Malak, *Appl. Surf. Sci*., 236 (2004)175

39. S. Umoren, I. Obot, E. Ebenso, *J. Chem*., 5 (2008)355.
40. R. Solmaz, *Corros*. *Sci*., 79 (2014) 169.
41. M. Quraishi, *Corros*. *Sci*., 70 (2013) 161.
42. R. Solmaz, *Corros*. *Sci*., 52 (2010)3321.
43. J. Aljourani, K. Raeissi, M. Golozar, *Corros. Sci*., 51 (2009)1836.
44. S.S. Zumdahl, *Chemistry, 3rd* Ed, D.C. Heath & Co. (1993) 645.
45. S. Abd El Wanees, A. Diab, O .Azazy, M.A. El Azim, *J. Disper. Sci. Techn*., 35 (2014) 1571.
46. S. Abd El Wanees, S.H. Seda, J. *Disper. Sci. Techn*., 40 (2019) 1813.
47. S. Abd El Wanees, M.I. Alahmdi, S.M. Rashwan, M.M. Kamel, and M.G. Abd Elsadek, *Int. J. Electrochem. Sci*., 11 (2016) 9265.